

# Uncertainty-Aware Collaborative System of Large and Small Models for Multimodal Sentiment Analysis

Shiqin Han<sup>1</sup>, Manning Gao<sup>2</sup>, Menghua Jiang<sup>1</sup>, Yuncheng Jiang<sup>1,2</sup>, Haifeng Hu<sup>3</sup>, Sijie Mai<sup>1\*</sup>

<sup>1</sup>School of Computer Science, South China Normal University, Guangzhou 510631, China

<sup>2</sup>School of Artificial Intelligence, South China Normal University, Guangzhou 510631, China

<sup>3</sup>School of Electronics and Information Technology, Sun Yat-sen University, Guangzhou 510275, China

20222121019@m.scnu.edu.cn, 20232005149@m.scnu.edu.cn, jiangmenghua@m.scnu.edu.cn, ycjiang@m.scnu.edu.cn, huhaif@mail.sysu.edu.cn, sijiemai@m.scnu.edu.cn

## Abstract

The advent of Multimodal Large Language Models (MLLMs) has significantly advanced the state-of-the-art in multimodal machine learning, yet their substantial computational demands present a critical barrier to real-world deployment. Conversely, smaller, specialized models offer high efficiency but often at the cost of performance. To reconcile this performance-efficiency trade-off, we propose a novel Uncertainty-Aware Collaborative System (U-ACS) that synergistically orchestrates a powerful MLLM (e.g., HumanOmni) and a lightweight baseline model for multimodal sentiment analysis. The core of our system is an uncertainty-driven cascade mechanism, where the efficient small model first acts as a rapid filter for all input samples. Only those samples yielding high predictive uncertainty, thereby indicating greater difficulty, are selectively escalated to the MLLM for more sophisticated analysis. Furthermore, our system introduces advanced strategies to handle ambiguous or conflicting predictions, including weighted averaging for predictions of similar polarity and a prompt-based cross-verification to resolve conflicting predictions when both models exhibit high uncertainty. This sample-difficulty-aware approach allows for a dynamic allocation of computational resources, drastically reducing inference costs while retaining the high accuracy of MLLM. Extensive experiments on benchmark datasets demonstrate that our proposed method achieves state-of-the-art performance, while requiring only a fraction of the computational resources compared to using a standalone MLLM.

## Introduction

The landscape of multimodal learning (Baltrušaitis, Ahuja, and Morency 2019) has been profoundly reshaped by the emergence of powerful Multimodal Large Language Models (MLLMs) such as HumanOmni (Zhao et al. 2025). Multimodal Sentiment Analysis (MSA), leveraging acoustic, textual, and visual information to predict human sentiment intensities and emotional states (Poria et al. 2017), can also benefit from the capability of MLLMs. With their vast parameter counts and sophisticated reasoning capabilities, MLLMs demonstrate an unparalleled ability to interpret complex, nuanced human expressions across textual, visual, and acoustic modalities. However, this remarkable ac-

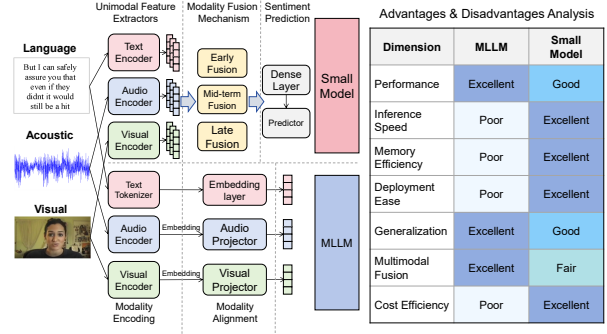


Figure 1: Advantages and limitations of existing approaches: small models offer efficiency but lack accuracy, while MLLMs provide high accuracy at heavy computational cost.

curacy comes at a significant cost. The substantial computational overhead associated with MLLMs poses a critical barrier to their deployment in many practical, real-world scenarios. This overhead manifests as high inference latency, significant memory requirements, and considerable energy consumption, particularly problematic where resources are constrained or real-time responses are paramount.

At the other end of the spectrum, there are smaller and specialized models (Wang et al. 2025a; Yu et al. 2021). These lightweight architectures are characterized by their computational efficiency, offering rapid inference speeds and minimal resource footprints. Yet, this efficiency is often achieved by sacrificing the deep, generalizable understanding inherent to MLLMs, resulting in a performance ceiling, particularly when confronted with ambiguous or out-of-distribution samples. This dichotomy presents a challenging trade-off for the field: a choice between the high accuracy of costly large models and the high efficiency of less capable small models. The pursuit of a solution that marries the strengths of both paradigms remains a significant and open research question.

To bridge this gap, we introduce a novel Uncertainty-Aware Collaborative System (U-ACS) that intelligently orchestrates the operations of a powerful MLLM and an efficient small baseline model. As conceptually illustrated in Figure 1, our approach is not a static ensemble but a fluid,

\*Corresponding author.

sample-aware cascade designed to achieve optimal performance with minimal average computational cost. The core principle is to allocate computational resources judiciously, reserving the analytical power of the MLLM exclusively for samples that genuinely require it.

The cornerstone of the proposed system is an uncertainty-guided routing mechanism. We posit that a model’s predictive uncertainty is a reliable proxy for sample difficulty (Tellamekala et al. 2024; Gao et al. 2024). Consequently, both the small models and MLLMs are trained to co-produce not only a sentiment prediction but also a quantifiable validation-calibrated measure of their own uncertainty. The inference process begins with the efficient small model, which acts as a rapid initial filter for all incoming samples. For a given sample, if the small model exhibits low uncertainty (i.e., high confidence), its prediction is accepted, and the process terminates. This ‘fast path’ effectively handles the majority of straightforward cases with minimal computational expense.

Only when the small model’s uncertainty exceeds a pre-defined threshold, indicating a ‘hard’ sample, is the inference process escalated to the MLLM. This selective escalation ensures that our most potent computational asset is used purposefully. Upon processing the sample, the MLLM also provides its prediction and uncertainty. If the MLLM is confident in its assessment, its superior judgment is adopted as the final result. However, the most intricate scenarios arise when the MLLM is also uncertain where both models produce predictions that require further deliberation. To resolve these problem, we introduce a sophisticated collaboration logic. When both models are confident and their predictions are similar in magnitude (e.g., both positive or both negative with comparable values), we employ a weighted average based on their uncertainty scores to refine the final prediction. In cases where the models produce conflicting sentiment polarities (e.g., one positive, one negative), we utilize a prompt-based cross-verification strategy, where both model’s predictions and uncertainties are incorporated into the MLLM’s prompt to stimulate re-evaluation and collaborative reasoning.

This hierarchical and adaptive approach allows our system to dynamically navigate the performance-cost landscape, delivering a solution that is both highly accurate and computationally tractable. Our main contributions can be summarized as follows:

- We propose a novel U-ACS that synthesizes a large, powerful MLLM with a small, efficient model to resolve the performance-versus-efficiency dilemma in MSA.
- We design an uncertainty-guided cascade mechanism that intelligently routes samples, significantly reducing average computational cost by reserving the MLLM for only the most challenging cases. We also design multiple strategies to estimate predictive uncertainty for challenging regression tasks.
- We introduce a sophisticated collaboration logic, including prompt-based cross-verification, to resolve predictive conflicts and ambiguities between two models.
- Through extensive experiments, we demonstrate that our

system achieves state-of-the-art performance on multiple MSA datasets while operating at a fraction of the computational cost of a standalone MLLM approach.

## Related Work

### Multimodal Sentiment Analysis

Early MSA research focused on feature fusion and representation learning techniques, ranging from simple concatenation and tensor-based methods (Zadeh et al. 2017; Liang et al. 2019) to attention-based mechanisms for capturing inter-modal dependencies (Tsai et al. 2019; Mai, Xing, and Hu 2021). In parallel, recent approaches have explored graph neural networks for modeling speaker-utterance relationships in conversational settings (Tu et al. 2024; Wang et al. 2025b) and self-supervised frameworks for handling incomplete or noisy data (Li et al. 2024). To improve efficiency beyond traditional Transformers, State Space Models like MSAMba (He et al. 2025) have demonstrated effective long-range modeling with lower computational complexity. However, these methods typically operate as monolithic systems, either prioritizing maximum performance or efficiency, without dynamic resource allocation mechanisms.

Large Language Models (LLMs) have catalyzed significant advances in MSA (Yang et al. 2024). These methods often use lightweight adapters like MSE-Adapter (Yang, Dong, and Qiang 2025) to enable multimodal capabilities in frozen LLMs while reducing training costs. More recently, Multimodal Large Language Models (MLLMs) have emerged, which can directly handle multimodal signals and project them into the feature space of LLMs and achieve better results (Zhao et al. 2025; Wu et al. 2025). While effective, these approaches invoke MLLMs for every sample, remaining computationally expensive for practical deployment.

### Collaboration of Large and Small Models

The concept of combining large, high-capacity models with small, efficient ones to optimize the performance-cost trade-off is an emerging trend in the broader machine learning community (Min et al. 2024; Chen, Zhao, and Han 2025). These model cascades use small models for easy cases and large models for complex inputs, successfully applied in computer vision and NLP tasks requiring low latency.

In the MSA domain, this collaborative paradigm is still nascent. The most related concepts can be found in knowledge distillation frameworks, where a larger “teacher” model’s knowledge is transferred to a smaller “student” model during training (Li et al. 2024). However, these methods focus on creating a single, more compact model for inference, rather than using both models dynamically during inference. To the best of our knowledge, a dynamic, uncertainty-driven cascade that synthesizes a massive MLLM with a specialized small model for MSA has not been explored. Our work is the first to propose such a framework, explicitly designed to balance the unparalleled accuracy of models like HumanOmni with the practical efficiency required for real-world applications.

## Methodology

### Problem Definition

The goal of MSA is to predict the sentiment intensity from given multimodal inputs. In the proposed U-ACS, we simultaneously incorporate three modalities: Text (T), Vision (V), and Audio (A). Each modality is represented by a tensor  $\hat{X}^m \in \mathbb{R}^{N_m \times d_m}$ , where  $N_m$  denotes the sequence length,  $d_m$  is the embedding dimension, and  $m \in \{T, V, A\}$  indicates the specific modality type.

### Overall Architecture

As shown in Figure 2, our proposed U-ACS synergistically integrates a lightweight small model (Uncertainty-aware Baseline Model, UBM) with a powerful MLLM through an uncertainty-guided cascade, consisting of three stages: **i**) In the first stage, the small model quickly processes all input samples, efficiently filtering out simple cases by making high-confidence predictions with minimal computational cost. **ii**) In the second stage, samples that exhibit higher predictive uncertainty are escalated to the LoRA-adapted MLLM, which performs more in-depth, modality-specific analysis to improve prediction accuracy. **iii**) In the third and final stage, the outputs from both models are combined through a collaborative reasoning mechanism, leveraging their complementary strengths to generate robust and reliable predictions, especially for the most complex cases.

### Small Model Filtering

The small model acts as the primary inference engine of the system, optimized for efficient multimodal learning and high-throughput processing. It delivers fast sentiment predictions for the majority of samples while generating reliable uncertainty estimates to guide sample routing within the cascade.

**Unimodal Learning** The model processes each modality using dedicated encoders. For the text modality, we extract the representation at the first time step:

$$\begin{aligned}\hat{\mathbf{X}}_t &= \text{TextEncoder}(\mathbf{U}_t; \theta_t) \in \mathbb{R}^{T \times d_t}, \\ \mathbf{x}_t &= \hat{\mathbf{X}}_t[0, :] \in \mathbb{R}^{d_t}\end{aligned}\quad (1)$$

For the acoustic and visual modalities, the last time step representation is extracted:

$$\begin{aligned}\hat{\mathbf{X}}_a &= \text{AudioEncoder}(\mathbf{U}_a; \theta_a) \in \mathbb{R}^{T \times d_a}, \\ \hat{\mathbf{X}}_v &= \text{VisualEncoder}(\mathbf{U}_v; \theta_v) \in \mathbb{R}^{T \times d_v}, \\ \mathbf{x}_a &= \hat{\mathbf{X}}_a[-1, :], \quad \mathbf{x}_v = \hat{\mathbf{X}}_v[-1, :]\end{aligned}\quad (2)$$

where  $\mathbf{x}_t$ ,  $\mathbf{x}_a$ , and  $\mathbf{x}_v$  represent the extracted feature vectors for the text, audio, and visual modalities, respectively.

**Multimodal Fusion and Prediction** The feature vectors  $\mathbf{x}_t$ ,  $\mathbf{x}_a$ , and  $\mathbf{x}_v$  are concatenated and fused for prediction:

$$\begin{aligned}\mathbf{h}_m &= \text{Fusion}(\mathbf{x}_t \| \mathbf{x}_a \| \mathbf{x}_v) \in \mathbb{R}^{d_m}, \\ \hat{y}_s &= \text{Predictor}(\mathbf{h}_m)\end{aligned}\quad (3)$$

where  $\text{Fusion}(\cdot)$  is a function that integrates the concatenated features into a fused representation of dimension  $d_m$ . The fused representation  $\mathbf{h}_m$  is then fed into a prediction function  $\text{Predictor}(\cdot)$  to produce the final sentiment score.

**Uncertainty Estimation** A critical requirement of our UBM is to reliably estimate predictive uncertainty, which is essential for making effective routing decisions. As MSA is a regression task, estimating its predictive uncertainty is actually very difficult. Here we put forward three simple and reasonable uncertainty estimation approaches for MSA :

(1) **Prediction-Truth Differences**, which employs an additional predictor to measure the absolute difference between predicted and true labels, treating larger differences as indicators of higher uncertainty. However, predicting label differences is very difficult, requiring the model to have full discriminative power to estimate the labels of all samples.

(2) **Ensemble Variance**, which trains multiple diverse predictors on different data subsets and uses the variance among their predictions as an uncertainty measure. Although this approach is theoretically sound, it introduces computational overhead because each input must be processed by multiple predictors, conflicting with our efficiency goals.

### (3) Our Method – Classification-based Entropy:

To overcome these limitations, we propose a classification-based entropy approach. Specifically, we transform the regression task into a three-class classification problem and employ a classifier to conduct the classification task, enabling the estimation of predictive uncertainty by computing the entropy of the output probability distribution. This method offers several key advantages: (i) computational efficiency achieved through a single forward pass; (ii) a principled, information-theoretic interpretation of uncertainty; and (iii) reducing the difficulty in uncertainty estimation, as the uncertainty of classification tasks is easier to estimate.

Specifically, alongside the primary regression predictor that outputs continuous sentiment scores  $\hat{y}_s$ , we introduce an auxiliary classifier. The continuous sentiment scores are discretized into three categories according to their polarity:

$$\text{class} = \begin{cases} 1 (\text{Negative}), & y < 0 \\ 0 (\text{Neutral}), & y = 0 \\ 2 (\text{Positive}), & y > 0 \end{cases}\quad (4)$$

The classification branch shares the same multimodal feature representation  $\mathbf{h}_m$  processed by the main regression predictor but employs a separate classifier:

$$\begin{aligned}\mathbf{z}_{cls} &= \text{Classifier}(\mathbf{h}_m), \\ p_s &= \text{Softmax}(\mathbf{z}_{cls}) = [p_1, p_2, p_3]\end{aligned}\quad (5)$$

where  $p_s$  denotes the predicted probability distribution over the three sentiment classes. The model is jointly optimized with a combined loss that integrates both regression and classification objectives:

$$\mathcal{L}_{sup} = \mathcal{L}_{reg}(\hat{y}_s, y) + \mathcal{L}_{cls}(p_s, y_{cls})\quad (6)$$

where  $\mathcal{L}_{reg}$  represents the Mean Squared Error (MSE) for regression,  $\mathcal{L}_{cls}$  is the Cross-Entropy (CE) loss for classification, and  $y_{cls}$  is the discretized ground truth label. During inference, uncertainty is quantified by the entropy of the predicted class distribution:

$$u_s = H(p_s) = - \sum_{i=1}^3 p_{s,i} \cdot \log(p_{s,i})\quad (7)$$

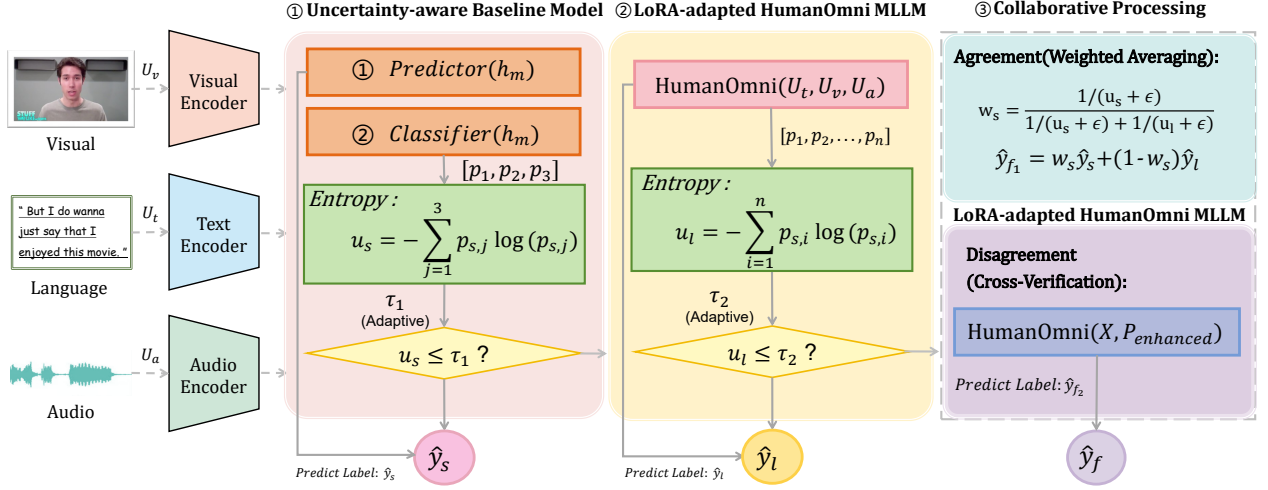


Figure 2: Three stages compose our U-ACS. The efficient baseline model acts as a primary filter, escalating only high-uncertainty samples to the MLLM (HumanOmni), followed by collaborative processing to resolve prediction conflicts.

where  $u_s$  denotes the uncertainty score,  $H(\cdot)$  is the entropy function, and  $p_{s,i}$  is the predicted probability of the  $i$ -th sentiment class. This entropy-based metric naturally reflects the model’s confidence: a high entropy value indicates greater uncertainty, corresponding to a more uniform distribution over classes, while a low entropy implies strong confidence concentrated on a single class (Xue et al. 2025).

## MLLM Refinement

We utilize HumanOmni (Yang, Dong, and Qiang 2025), a 7-billion-parameter MLLM, as the expert oracle for handling difficult samples. The model’s output is formulated as:

$$\hat{y}_l = \text{HumanOmni}(\mathbf{U}_t, \mathbf{U}_a, \mathbf{U}_v) \quad (8)$$

where  $\mathbf{U}_t, \mathbf{U}_a, \mathbf{U}_v$  denote the input features from text, audio, and visual modalities, respectively, and  $\hat{y}_l$  is the predicted sentiment score. To efficiently adapt HumanOmni to our task, we apply Low-Rank Adaptation (LoRA) (Hu et al. 2022), which decomposes the weight update into low-rank matrices  $A \in \mathbb{R}^{d \times r}$  and  $B \in \mathbb{R}^{r \times d}$ , with rank  $r$  much smaller than  $d$ . The adapted weight matrix is given by  $W_{\text{new}} = W + AB$ , where  $W$  is the original weight matrix and only  $A$  and  $B$  are trainable during fine-tuning. The MLLM then outputs a probability distribution over the possible sentiment classes, computed as:

$$\mathbf{p}_l = \text{Softmax}(\text{logits}_l) = [p_1, p_2, \dots, p_n], \quad (9)$$

where  $\mathbf{p}_l$  represents the predicted probability vector,  $p_i$  is the probability of the  $i$ -th class, and  $n$  is the total number of sentiment classes. We quantify uncertainty by calculating the entropy of this distribution:

$$u_l = H(\mathbf{p}_l) = -\sum_{i=1}^n p_{l,i} \cdot \log(p_{l,i}), \quad (10)$$

where  $u_l$  denotes the uncertainty score and  $H(\cdot)$  is the entropy function. Higher entropy corresponds to higher uncertainty, providing a principled confidence measure for the

model’s predictions. As output consists of multiple tokens, we average the uncertainties of all label-related output tokens to obtain the final uncertainty.

## Uncertainty Threshold Estimation

We adopt a principled statistical approach to determine the uncertainty thresholds for both the small model and the MLLM. This method analyzes the uncertainty distributions on the validation set, providing a theoretically grounded yet computationally efficient way to select thresholds.

The threshold selection procedure is applied consistently to both models. For each model, we partition the validation samples into two groups based on whether the model’s predicted polarity matches the ground truth. We define  $\mathbb{D}_{\text{same}}$  as the set of samples where the prediction and ground truth share the same polarity (both positive or both negative), and  $\mathbb{D}_{\text{opposite}}$  as the set where they differ in polarity. For each group, we fit a Gaussian distribution to the uncertainty values and compute the corresponding mean uncertainties:

$$\begin{aligned} \mu_{\text{same}} &= \mathbb{E}_i[(u)_i \mid i \in \mathbb{D}_{\text{same}}], \\ \mu_{\text{opposite}} &= \mathbb{E}_i[(u)_i \mid i \in \mathbb{D}_{\text{opposite}}] \end{aligned} \quad (11)$$

where  $(u)_i$  denotes the uncertainty for sample  $i$ , and the means are estimated via Gaussian fitting on the validation set. Finally, we apply this method with Gaussian fitting to compute the specific thresholds for both models:

$$\begin{aligned} \tau_1 &= (1 - \lambda) \cdot \mu_{\text{same}}^{(s)} + \lambda \cdot \mu_{\text{opposite}}^{(s)} + \beta, \\ \tau_2 &= (1 - \lambda) \cdot \mu_{\text{same}}^{(l)} + \lambda \cdot \mu_{\text{opposite}}^{(l)} + \beta, \end{aligned} \quad (12)$$

where  $\tau_1$  corresponds to UBM and  $\tau_2$  to the MLLM. The superscripts  $(s)$  and  $(l)$  denote statistics computed from UBM and MLLM predictions, respectively.  $\lambda$  is a hyperparameter for weight with a default value of 0.5, while  $\beta$  is a hyperparameter for bias with a default value of 0.0.

## Summary of U-ACS

Building upon the uncertainty thresholds  $\tau_1$  and  $\tau_2$ , we now present the overall inference workflow, which is shown in

Algorithm 1. This workflow employs a dynamic collaboration strategy that sequentially leverages UBM and MLLM, guided by their uncertainty estimates, to efficiently and accurately produce the final prediction. The process proceeds through three stages:

**Stage 1: Small Model Filtering.** Compute the baseline prediction  $\hat{y}_s$  and uncertainty  $u_s$ . If the uncertainty is below the adaptive validation-calibrated threshold  $\tau_1$ , accept this prediction directly. Otherwise, proceed to the MLLM Refinement Stage:

$$\hat{y} = \begin{cases} \hat{y}_s, & u_s \leq \tau_1 \\ \text{Proceed to Stage 2, } u_s > \tau_1 \end{cases} \quad (13)$$

**Stage 2: MLLM Refinement.** For samples with higher uncertainty, invoke the MLLM to obtain prediction  $\hat{y}_l$  along with its uncertainty  $u_l$ . Accept the prediction if the uncertainty is below the second threshold  $\tau_2$ :

$$\hat{y} = \begin{cases} \hat{y}_l, & u_l \leq \tau_2 \\ \text{Proceed to Stage 3, } u_l > \tau_2 \end{cases} \quad (14)$$

**Stage 3: Collaborative Reasoning.** For cases still deemed highly uncertain, apply collaborative strategies based on whether two models agree on sentiment polarity:

- *Agreement (Weighted Averaging):* If both models predict the same polarity, compute adaptive weights based on uncertainty and combine their outputs:

$$w_s = \frac{1/(u_s + \epsilon)}{1/(u_s + \epsilon) + 1/(u_l + \epsilon)}, \quad (15)$$

$$\hat{y} = w_s \cdot \hat{y}_s + (1 - w_s) \cdot \hat{y}_l$$

- *Disagreement (Cross-Verification):* If two models disagree, augment the prompt with previous predictions and uncertainties, and re-predict through the MLLM:

$$\hat{y} = \text{HumanOmni}(X, P_{\text{enhanced}}) \quad (16)$$

where  $P_{\text{enhanced}}$  provides richer context by including UBM’s prediction  $\hat{y}_s$  and uncertainty  $u_s$ , along with the prediction and uncertainty of the MLLM.

## Experiments

U-ACS has been evaluated using the CMU-MOSI (MOSI) (Zadeh et al. 2016), CMU-MOSEI (MOSEI) (Zadeh et al. 2018), and CH-SIMS v1 (SIMS) (Yu et al. 2020) datasets. Due to space constraints, introductions to the experimental settings, baselines, evaluation metrics, and descriptions of the datasets are provided in the supplementary material.

## Experiment Results

To assess the performance of U-ACS, we utilized three well-recognized MSA datasets. As presented in Table 1, U-ACS demonstrates superior performance, achieving state-of-the-art results in some evaluation metrics while maintaining computational efficiency. Compared to HumanOmni, U-ACS achieves 0.5 points improvement in Acc2 and F1 score on MOSI. For MOSEI, U-ACS achieves 0.3 points improvement in Acc2 and 0.4 points improvement in F1 score. Table 2 presents the robustness validation results of

---

## Algorithm 1: Uncertainty-Aware Collaborative Inference

---

**Input:** Sample  $X = (U_t, U_a, U_v)$ , Small model  $M_s$ , MLLM  $M_l$ , uncertainty thresholds  $\tau_1, \tau_2$ ;  
**Output:** Final prediction  $\hat{y}$ ;

- 1:  $\hat{y}_s, \mathbf{p}_s \leftarrow M_s(X);$
- 2:  $u_s \leftarrow -\sum_{i=1}^3 p_{s,i} \cdot \log p_{s,i};$
- 3: **if**  $u_s \leq \tau_1$  **then**
- 4:    $\hat{y} \leftarrow \hat{y}_s;$
- 5: **else**
- 6:    $\hat{y}_l, \mathbf{p}_l \leftarrow M_l(X);$
- 7:    $u_l \leftarrow -\sum_{i=1}^n p_{l,i} \cdot \log(p_{l,i});$
- 8:   **if**  $u_l \leq \tau_2$  **then**
- 9:      $\hat{y} \leftarrow \hat{y}_l;$
- 10:   **else**
- 11:     **if**  $\hat{y}_s$  and  $\hat{y}_l$  are the same polarity **then**
- 12:        $w_s \leftarrow \frac{1/(u_s + \epsilon)}{1/(u_s + \epsilon) + 1/(u_l + \epsilon)};$
- 13:        $\hat{y} \leftarrow w_s \cot \hat{y}_s + (1 - w_s) \cdot \hat{y}_l;$
- 14:     **else**
- 15:       Construct  $P_{\text{enhanced}}$  from  $\hat{y}_s, u_s, \hat{y}_l, u_l$ ;
- 16:        $\hat{y} \leftarrow M_l(X, P_{\text{enhanced}});$
- 17:     **end if**
- 18:     **return**  $\hat{y};$
- 19:   **end if**
- 20: **end if**

---

U-ACS in cross-lingual scenarios. On the Chinese dataset CH-SIMS v1, the model maintains leading performance across most metrics, including Acc3, Acc2 and F1 score. Furthermore, U-ACS significantly outperforms traditional multimodal methods, demonstrating the effectiveness of uncertainty-guided collaboration across different languages and data characteristics.

Notably, compared with HumanOmni, our method achieves the optimal performance in the Acc2 metric across three datasets. The superiority of the Acc2 performance is attributed to the design of the model in terms of threshold setting. We explicitly divide samples into same and opposite categories according to the coarse-grained positive and negative categories, which is highly consistent with the computational logic of Acc2. Moreover, in the small model UBM, we transform continuous sentiment labels into positive, negative, and neutral classes. These designs make the optimization of Acc2 (positive versus negative) more targeted, thereby highlighting significant advantages.

## Study on Computational Efficiency

Table 3 compares the computational costs, Acc2, and MAE of different approaches. Compared with HumanOmni, our strategy achieves the optimal performance in the Acc2 metric on MOSI, MOSEI, and SIMS datasets, while attaining significant efficiency improvements. Specifically, on the MOSI dataset, the runtime of ours is only 33% of that of the HumanOmni, which significantly reduces the inference time while maintaining the performance. These results indicate that, our strategy, while ensuring that the model performance reaches the level of MLLM, has significantly shortened inference time and reduced model complexity, greatly

Method	CMU-MOSI					CMU-MOSEI				
	Acc7↑	Acc2↑	F1↑	MAE↓	Corr↑	Acc7↑	Acc2↑	F1↑	MAE↓	Corr↑
MISA (Hazarika, Zimmermann, and Poria 2020)	42.3	83.4	83.6	0.783	0.761	52.2	85.5	85.3	0.555	0.756
DBM (Yu et al. 2021)	45.6	84.5	84.4	0.719	0.794	53.7	84.8	84.7	0.535	0.761
<i>LMF</i> ( <i>Liuet et al. 2018</i> ) <sup>†</sup>	33.8	79.2	79.2	0.950	0.651	51.6	83.5	83.4	0.575	0.716
<i>MulT</i> ( <i>Tsai et al. 2019</i> ) <sup>†</sup>	36.9	79.7	79.6	0.879	0.702	52.8	84.6	84.5	0.559	0.733
MAG-BERT (Rahman et al. 2020)	43.6	84.4	84.6	0.727	0.781	52.7	84.8	84.7	0.543	0.755
Self-MM (Yu et al. 2021)	45.8	84.9	84.8	0.731	0.785	53.0	85.2	85.2	0.540	0.763
ConFEDE (Yang et al. 2023)	42.3	85.5	85.5	0.742	0.784	54.9	85.8	85.8	0.522	0.780
DLF (Wang et al. 2025a)	47.1	85.1	85.0	0.731	0.781	53.9	85.4	85.3	0.536	0.764
DEVA (Wu et al. 2025)	46.3	86.3	86.3	0.730	0.787	52.3	86.1	<b>86.2</b>	0.541	0.769
HumanOmni (Zhao et al. 2025)	<b>52.8</b>	<u>91.3</u>	<u>91.3</u>	<b>0.549</b>	<b>0.881</b>	<b>58.6</b>	<u>86.1</u>	85.4	<b>0.483</b>	<b>0.807</b>
<b>U-ACS</b>	<u>51.2</u>	<b>91.8</b>	<b>91.8</b>	0.585	0.868	55.4	<b>86.4</b>	85.8	0.506	0.784

Table 1: Performance comparison on CMU-MOSI and CMU-MOSEI datasets. Best results are in **bold**, second-best are underlined. <sup>†</sup> means the results are from (Feng et al. 2024).

Method	CH-SIMS v1					
	Acc5↑	Acc3↑	Acc2↑	F1↑	MAE↓	Corr↑
MISA	-	-	76.5	76.6	0.447	0.563
DBM	41.5	65.5	80.0	80.4	0.425	0.595
<i>TFN</i> <sup>†</sup>	39.3	65.1	78.4	78.6	0.432	0.591
<i>MulT</i> <sup>†</sup>	37.9	64.8	78.6	79.7	0.453	0.564
MAG-BERT	-	-	74.4	71.8	0.492	0.399
DEVA	43.1	65.4	79.6	80.3	0.424	0.583
<i>KuDA</i> <sup>†</sup>	43.5	66.5	80.7	80.7	0.408	0.613
HumanOmni	<b>52.1</b>	<u>72.9</u>	<u>85.1</u>	<u>85.0</u>	<b>0.327</b>	<b>0.749</b>
<b>U-ACS</b>	<u>51.0</u>	<b>73.1</b>	<b>85.8</b>	<b>85.1</b>	0.354	0.691

Table 2: Performance comparison on CH-SIMS v1 dataset. Best results are in **bold**, second-best are underlined. <sup>†</sup> means the results are from (Feng et al. 2024).

Dataset	Method	Runtime↓	Acc2↑	MAE↓
CMU-MOSI	UBM	<b>15.35</b>	86.1	0.716
	HumanOmni	379.18	<u>91.3</u>	<b>0.549</b>
	<b>Ours</b>	<u>125.76</u>	<b>91.8</b>	<u>0.585</u>
CMU-MOSEI	UBM	<b>35.02</b>	86.3	0.527
	HumanOmni	9815.56	86.1	<b>0.483</b>
	<b>Ours</b>	<u>5561.18</u>	<b>86.4</b>	0.506
CH-SIMS v1	UBM	<b>18.76</b>	80.5	0.409
	HumanOmni	470.61	<u>85.1</u>	<b>0.327</b>
	<b>Ours</b>	<u>260.58</u>	<b>85.8</b>	0.354

Table 3: Computational efficiency comparison. Time is measured in seconds per sample. Best results are in **bold**, second-best are underlined.

improving operational efficiency and ultimately achieving a balance between performance and efficiency.

### Study on Uncertainty Distributions

To determine optimal uncertainty thresholds  $\tau_1$  and  $\tau_2$ , We fit the uncertainty of correctly predicted samples and incorrectly predicted samples to a Gaussian distribution. Figure 3 shows the uncertainty distributions for correct and incorrect predictions on CMU-MOSI testing set. Although there is an overlap in the uncertainties of some samples, the uncertainty distributions of correctly predicted samples and incorrectly predicted samples on the MOSI dataset still show significant differences. The visualization indicates the effectiveness of

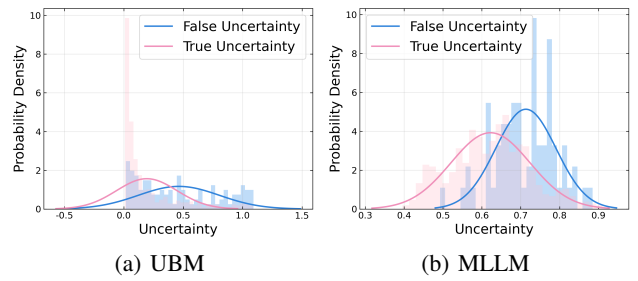


Figure 3: The distribution of uncertainties on CMU-MOSI.

the proposed uncertainty estimation method (especially for UBM whose uncertainty is hard to estimate). Consequently, effective classification of the two types of samples can be achieved by calculating thresholds.

### Case Study

To illustrate the effectiveness of our strategy, we present a case study on a challenging sample from the CH-SIMS dataset. Figure 4 demonstrates how our framework processes a complex sentiment analysis case where individual models struggle but collaboration system succeeds.

The selected sample contains ambiguous multimodal cues: nuanced textual content discussing career limitations, subtle facial expressions, and calm acoustic tone. This complexity causes the UBM to predict neutral sentiment ( $\hat{y}_s = 0.0$ ) with high uncertainty ( $u_s = 1.10 > \tau_1 = 0.59$ ), correctly triggering escalation. The MLLM provides better polarity detection ( $\hat{y}_l = -0.2$ ) but still exhibits uncertainty above the threshold ( $u_l = 0.51 > \tau_2 = 0.48$ ), leading to collaborative processing. Since the predictions have conflicting polarities (neutral vs. negative), the cross-verification mechanism is activated, prompting a second MLLM inference that successfully achieves final prediction ( $\hat{y}_f = -0.5$ ) with improved accuracy relative to the ground truth ( $-0.4$ ).

This case demonstrates three key advantages. Firstly, uncertainty-guided routing prevents incorrect fast-path decisions when the baseline model faces ambiguous inputs. Secondly, the framework effectively handles polarity conflicts between models through cross-verification. Thirdly, the col-

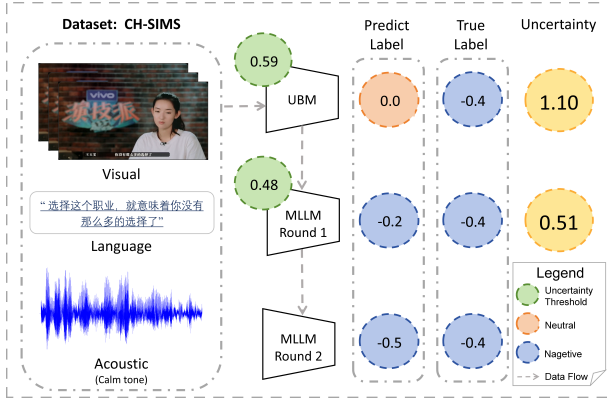


Figure 4: Case study on a challenging sample. UBM predicts neutral with high uncertainty triggering escalation. The MLLM first predicts with a uncertainty exceeding the threshold. A second MLLM run is activated for cross-verification, yielding a final and more precise prediction.

Dataset	Description	Acc7	Acc2	MAE
MOSI	W/o Cross-Verification	50.4	<u>90.4</u>	0.631
	W/o Uncertainty	<b>51.7</b>	89.6	<u>0.600</u>
	Prediction-Truth Difference	46.7	87.0	0.649
	Ensemble Variance	46.9	88.7	0.632
	<b>Ours</b>	<u>51.2</u>	<b>91.8</b>	<b>0.585</b>
SIMS	W/o Cross-Verification	<u>50.1</u>	<u>85.1</u>	0.358
	W/o Uncertainty	47.9	83.6	0.357
	Prediction-Truth Difference	45.7	81.2	0.407
	Ensemble Variance	41.8	78.1	0.398
	<b>Ours</b>	<b>51.0</b>	<b>85.8</b>	<b>0.354</b>

Table 4: Ablation experiments on CMU-MOSI and CH-SIMS. Best results are in **bold**, second-best are underlined.

laborative approach achieves superior accuracy on challenging samples .

### Ablation Studies

We conduct comprehensive ablation studies to validate each component of our framework. Table 4 presents the results:

**(1) Uncertainty Routing Mechanism:** In ‘W/O Uncertainty’, we randomly select identical samples for processing by the MLLM, rather than selecting samples based on uncertainty. Removing the uncertainty routing mechanism significantly degrades performance (the Acc2 drops by 2.2 points and MAE also drops significantly on both datasets). The Acc5 also decreases by 3.1 points on SIMS, demonstrating the critical importance of sample routing mechanism. This is because uncertainty can reflect the confidence of model prediction, and samples of high uncertainty are often hard samples that should be processed more advanced models.

**(2) Cross-verification Strategies:** Although only a few samples will activate the cross-verification mechanism, it proves essential for optimal performance. Without it, Acc2 decreases by 1.4 points on MOSI and 0.7 points on SIMS, while MAE also deteriorates significantly, confirming the effectiveness of cross-verification. This is because cross-verification can effectively handle the hardest samples that

cannot be well identified by individual models.

**(3) Uncertainty Quantification Methods:** Our entropy-based approach substantially outperforms alternative uncertainty estimation methods. Compared to prediction-truth difference, we achieve 4.8-point improvements in Acc2 on MOSI and 4.6-point improvements on SIMS. Ensemble variance performs even worse, particularly on SIMS with a 7.7-point Acc2 gap and 9.2-point Acc5 gap. These results confirm that our single-pass entropy computation provides both efficiency and effectiveness for uncertainty estimation, which cleverly circumvents the issue of difficulty in computing uncertainty for regression task via transforming regression task into classification task.

### Conclusion

We propose a novel method named U-ACS to combine traditional multimodal models with MLLMs to address the imbalance between performance and efficiency in MSA. U-ACS explicitly computes the uncertainty of traditional models and MLLM, designing an uncertainty-driven cascade mechanism to select samples yielding high predictive uncertainty for processing by the MLLM. We also propose advanced collaboration strategies to handle the hardest samples. U-ACS significantly improves efficiency of MLLM while ensuring model performance.

## References

Baltrušaitis, T.; Zadeh, A.; Lim, Y. C.; and Morency, L.-P. 2018. Openface 2.0: Facial behavior analysis toolkit. In *2018 13th IEEE international conference on automatic face & gesture recognition (FG 2018)*, 59–66. IEEE.

Baltrušaitis, T.; Ahuja, C.; and Morency, L.-P. 2019. Multimodal Machine Learning: A Survey and Taxonomy. *IEEE Transactions on Pattern Analysis and Machine Intelligence*, 41(2): 423–443.

Chen, Y.; Zhao, J.; and Han, H. 2025. A survey on collaborative mechanisms between large and small language models. *arXiv preprint arXiv:2505.07460*.

Degottex, G.; Kane, J.; Drugman, T.; Raitio, T.; and Scherer, S. 2014. COVAREP: A Collaborative Voice Analysis Repository for Speech Technologies. In *ICASSP*, 960–964.

Feng, X.; Lin, Y.; He, L.; Li, Y.; Chang, L.; and Zhou, Y. 2024. Knowledge-Guided Dynamic Modality Attention Fusion Framework for Multimodal Sentiment Analysis. In Al-Onaizan, Y.; Bansal, M.; and Chen, Y.-N., eds., *Findings of the Association for Computational Linguistics: EMNLP 2024*, 14755–14766. Miami, Florida, USA: Association for Computational Linguistics.

Gao, Z.; Jiang, X.; Xu, X.; Shen, F.; Li, Y.; and Shen, H. T. 2024. Embracing Unimodal Aleatoric Uncertainty for Robust Multimodal Fusion. In *Proceedings of the IEEE/CVF Conference on Computer Vision and Pattern Recognition*, 26876–26885.

Hazarika, D.; Zimmermann, R.; and Poria, S. 2020. MISA: Modality-Invariant and -Specific Representations for Multimodal Sentiment Analysis. *Proceedings of the 28th ACM International Conference on Multimedia*.

He, X.; Liang, H.; Peng, B.; Xie, W.; Khan, M. H.; Song, S.; and Yu, Z. 2025. MSAMba: Exploring Multimodal Sentiment Analysis with State Space Models. *Proceedings of the AAAI Conference on Artificial Intelligence*, 39(2): 1309–1317.

Hu, E. J.; Shen, Y.; Wallis, P.; Allen-Zhu, Z.; Li, Y.; Wang, S.; Wang, L.; Chen, W.; et al. 2022. Lora: Low-rank adaptation of large language models. *ICLR*, 1(2): 3.

Li, M.; Yang, D.; Lei, Y.; Wang, S.; Wang, S.; Su, L.; Yang, K.; Wang, Y.; Sun, M.; and Zhang, L. 2024. A Unified Self-Distillation Framework for Multimodal Sentiment Analysis with Uncertain Missing Modalities. *Proceedings of the AAAI Conference on Artificial Intelligence*, 38(9): 10074–10082.

Liang, P. P.; Liu, Z.; Tsai, Y.-H. H.; Zhao, Q.; Salakhutdinov, R.; and Morency, L.-P. 2019. Learning Representations from Imperfect Time Series Data via Tensor Rank Regularization. In *ACL*, 1569–1576.

Liu, Z.; Shen, Y.; Lakshminarasimhan, V. B.; Liang, P. P.; Bagher Zadeh, A.; and Morency, L.-P. 2018. Efficient Low-rank Multimodal Fusion With Modality-Specific Factors. In Gurevych, I.; and Miyao, Y., eds., *Proceedings of the 56th Annual Meeting of the Association for Computational Linguistics (Volume 1: Long Papers)*, 2247–2256. Melbourne, Australia: Association for Computational Linguistics.

Mai, S.; Xing, S.; and Hu, H. 2021. Analyzing Multimodal Sentiment Via Acoustic- and Visual-LSTM With Channel-Aware Temporal Convolution Network. *IEEE/ACM Transactions on Audio, Speech, and Language Processing*, 29: 1424–1437.

McFee, B.; Raffel, C.; Liang, D.; Ellis, D. P.; McVicar, M.; Battenberg, E.; and Nieto, O. 2015. librosa: Audio and music signal analysis in python. In *Proceedings of the 14th python in science conference*, volume 8, 18–25.

Min, Q.; Guo, Q.; Hu, X.; Huang, S.; Zhang, Z.; and Zhang, Y. 2024. Synergetic event understanding: A collaborative approach to cross-document event coreference resolution with large language models. *arXiv preprint arXiv:2406.02148*.

Poria, S.; Cambria, E.; Bajpai, R.; and Hussain, A. 2017. A review of affective computing: From unimodal analysis to multimodal fusion. *Information Fusion*, 37: 98–125.

Rahman, W.; Hasan, M. K.; Lee, S.; Bagher Zadeh, A.; Mao, C.; Morency, L.-P.; and Hoque, E. 2020. Integrating Multimodal Information in Large Pretrained Transformers. In Jurafsky, D.; Chai, J.; Schluter, N.; and Tetreault, J., eds., *Proceedings of the 58th Annual Meeting of the Association for Computational Linguistics*, 2359–2369. Online: Association for Computational Linguistics.

Tellamekala, M. K.; Amiriparian, S.; Schuller, B. W.; André, E.; Giesbrecht, T.; and Valstar, M. 2024. COLD Fusion: Calibrated and Ordinal Latent Distribution Fusion for Uncertainty-Aware Multimodal Emotion Recognition. *IEEE Transactions on Pattern Analysis and Machine Intelligence*, 46(2): 805–822.

Tsai, Y.-H. H.; Bai, S.; Liang, P. P.; Kolter, J. Z.; Morency, L.-P.; and Salakhutdinov, R. 2019. Multimodal Transformer for Unaligned Multimodal Language Sequences. In Korhonen, A.; Traum, D.; and Márquez, L., eds., *Proceedings of the 57th Annual Meeting of the Association for Computational Linguistics*, 6558–6569. Florence, Italy: Association for Computational Linguistics.

Tu, G.; Xie, T.; Liang, B.; Wang, H.; and Xu, R. 2024. Adaptive Graph Learning for Multimodal Conversational Emotion Detection. *Proceedings of the AAAI Conference on Artificial Intelligence*, 38(17): 19089–19097.

Wang, P.; Zhou, Q.; Wu, Y.; Chen, T.; and Hu, J. 2025a. DLF: Disentangled-language-focused multimodal sentiment analysis. In *Proceedings of the AAAI Conference on Artificial Intelligence*, volume 39, 21180–21188.

Wang, Y.; Fang, X.; Yin, H.; Li, D.; Li, G.; Xu, Q.; Xu, Y.; Zhong, S.; and Xu, M. 2025b. BIG-FUSION: Brain-Inspired Global-Local Context Fusion Framework for Multimodal Emotion Recognition in Conversations. *Proceedings of the AAAI Conference on Artificial Intelligence*, 39(2): 1574–1582.

Wu, S.; He, D.; Wang, X.; Wang, L.; and Dang, J. 2025. Enriching multimodal sentiment analysis through textual emotional descriptions of visual-audio content. In *Proceedings of the AAAI Conference on Artificial Intelligence*, volume 39, 1601–1609.

Xue, B.; Mi, F.; Zhu, Q.; Wang, H.; Wang, R.; Wang, S.; Yu, E.; Hu, X.; and Wong, K.-F. 2025. Ualign: Leveraging uncertainty estimations for factuality alignment on large language models. In *ACL*.

Yang, H.; Zhao, Y.; Wu, Y.; Wang, S.; Zheng, T.; Zhang, H.; Ma, Z.; Che, W.; and Qin, B. 2024. Large language models meet text-centric multimodal sentiment analysis: A survey. *arXiv preprint arXiv:2406.08068*.

Yang, J.; Yu, Y.; Niu, D.; Guo, W.; and Xu, Y. 2023. ConFEDE: Contrastive Feature Decomposition for Multimodal Sentiment Analysis. In Rogers, A.; Boyd-Graber, J.; and Okazaki, N., eds., *Proceedings of the 61st Annual Meeting of the Association for Computational Linguistics (Volume 1: Long Papers)*, 7617–7630. Toronto, Canada: Association for Computational Linguistics.

Yang, Y.; Dong, X.; and Qiang, Y. 2025. MSE-Adapter: A Lightweight Plugin Endowing LLMs with the Capability to Perform Multimodal Sentiment Analysis and Emotion Recognition. *arXiv:2502.12478*.

Yu, W.; Xu, H.; Meng, F.; Zhu, Y.; Ma, Y.; Wu, J.; Zou, J.; and Yang, K. 2020. CH-SIMS: A Chinese Multimodal Sentiment Analysis Dataset with Fine-grained Annotation of Modality. In Jurafsky, D.; Chai, J.; Schluter, N.; and Tetreault, J., eds., *Proceedings of the 58th Annual Meeting of the Association for Computational Linguistics*, 3718–3727. Online: Association for Computational Linguistics.

Yu, W.; Xu, H.; Yuan, Z.; and Wu, J. 2021. Learning modality-specific representations with self-supervised multi-task learning for multimodal sentiment analysis. In *Proceedings of the AAAI conference on artificial intelligence*, volume 35, 10790–10797.

Zadeh, A.; Chen, M.; Poria, S.; Cambria, E.; and Morency, L.-P. 2017. Tensor Fusion Network for Multimodal Sentiment Analysis. In Palmer, M.; Hwa, R.; and Riedel, S., eds., *Proceedings of the 2017 Conference on Empirical Methods in Natural Language Processing*, 1103–1114. Copenhagen, Denmark: Association for Computational Linguistics.

Zadeh, A.; Liang, P. P.; Poria, S.; Cambria, E.; and philippe Morency, L. 2018. Multimodal Language Analysis in the Wild: CMU-MOSEI Dataset and Interpretable Dynamic Fusion Graph. In *Annual Meeting of the Association for Computational Linguistics*.

Zadeh, A.; Zellers, R.; Pincus, E.; and Morency, L.-P. 2016. MOSI: Multimodal Corpus of Sentiment Intensity and Subjectivity Analysis in Online Opinion Videos. *arXiv:1606.06259*.

Zhang, K.; Zhang, Z.; Li, Z.; and Qiao, Y. 2016. Joint Face Detection and Alignment Using Multitask Cascaded Convolutional Networks. *IEEE Signal Processing Letters*, 23(10): 1499–1503.

Zhao, J.; Yang, Q.; Peng, Y.; Bai, D.; Yao, S.; Sun, B.; Chen, X.; Fu, S.; chen, W.; Wei, X.; and Bo, L. 2025. HumanOmni: A Large Vision-Speech Language Model for Human-Centric Video Understanding. *arXiv:2501.15111*.

## Appendix

### Datasets

We evaluate our Uncertainty-Aware Collaborative System (U-ACS) on three widely used multimodal sentiment analysis benchmarks: CMU-MOSI, CMU-MOSEI, and CH-SIMS v1. Each dataset presents unique characteristics and challenges for multimodal sentiment analysis.

- **CMU-MOSI** (Zadeh et al. 2016) contains 2,199 video segments that study the interaction patterns between facial gestures and spoken words for sentiment prediction. The dataset provides fine-grained sentiment annotations on a continuous scale from strongly negative to strongly positive, making it ideal for evaluating both regression and classification capabilities of multimodal models.
- **CMU-MOSEI** (Zadeh et al. 2018) is a larger multimodal dataset for sentiment analysis and emotion recognition, containing 23,453 annotated video segments from 1,000 distinct speakers across 250 topics, serving as the next generation expansion of MOSI. The dataset’s scale and diversity provide a robust evaluation platform for assessing model generalization across different speakers and topics.
- **CH-SIMS v1** (Yu et al. 2020) is a Chinese multimodal dataset which contains 2,281 refined video segments in the wild with both multimodal and independent unimodal annotation. This dataset enables cross-lingual validation of our approach and demonstrates the framework’s robustness across different languages and cultural contexts.

### Evaluation Metrics

Following standard multimodal sentiment analysis (MSA) evaluation protocols, we report comprehensive performance metrics across different granularities:

#### Classification Metrics:

- **7-class accuracy (Acc7):** Accuracy for fine-grained sentiment classification across seven sentiment levels, evaluating the model’s ability to distinguish subtle sentiment differences.
- **Binary accuracy (Acc2):** Accuracy for positive/negative classification, which is crucial for practical applications requiring simple sentiment polarity detection.
- **F1-score:** Harmonic mean of precision and recall for binary classification, providing a balanced measure that accounts for both false positives and false negatives.
- **5-class accuracy (Acc5):** Used specifically for CH-SIMS dataset, evaluating performance on five sentiment categories.
- **3-class accuracy (Acc3):** Used for CH-SIMS dataset, assessing performance on positive, negative, and neutral sentiment categories.

#### Regression Metrics:

- **Mean Absolute Error (MAE):** Measures the average absolute difference between predicted and ground truth sentiment scores, providing insight into prediction precision.

- **Pearson correlation (Corr):** Evaluates the linear correlation between predictions and ground truth, indicating how well the model captures sentiment intensity relationships.

#### Efficiency Metrics:

- **Inference Time:** Runtime measured in seconds to assess computational efficiency.

## B Uncertainty-aware Baseline Model (UBM) Architecture

This section provides detailed information about the architecture of UBM, which serves as the efficient filtering component in our U-ACS framework.

### Overall UBM Architecture

The UBM is built upon a multimodal sentiment analysis framework with key modifications to support uncertainty estimation and improve multimodal fusion capabilities. The model consists of three main components: modality-specific encoders, multimodal fusion mechanisms, and dual prediction heads (regression and classification).

### Feature Extraction

(1) **Visual Modality:** For the CMU-MOSI and CMU-MOSEI datasets, following our baseline Self-MM (Yu et al. 2021), Facet<sup>1</sup> is utilized to extract a collection of visual features, which include facial action units, facial landmarks, head pose, gaze tracking, and histogram of oriented gradients (HOG) features, among others. These visual features are extracted from each utterance at a rate of 30Hz, resulting in a temporal sequence of facial gestures. For the CH-SIMS dataset, MTCNN face detection algorithm (Zhang et al. 2016) is first applied to obtain aligned faces. Subsequently, the MultiComp OpenFace2.0 toolkit (Baltrusaitis et al. 2018) is employed to extract a set of 68 facial landmarks, 17 facial action units, head pose, head orientation, and eye gaze, among other features.

(2) **Acoustic Modality:** For the CMU-MOSI and CMU-MOSEI datasets, audio analysis framework COVAREP (De-gottex et al. 2014) is employed to extract acoustic features. These features include 12 Mel-frequency cepstral coefficients, pitch tracking, speech polarity, glottal closure instants, spectral envelope, peak slope parameters, and maxima dispersion quotients, among others. The acoustic features are extracted from the full audio clip of each utterance at a sampling rate of 100Hz, forming a sequence that captures variations in the tone of voice throughout the utterance. For the CH-SIMS dataset, LibROSA (McFee et al. 2015) speech toolkit, configured with default parameters, is utilized to extract acoustic features at a sampling rate of 22,050Hz. The extracted features consist of 33-dimensional frame-level acoustic features, which include 1-dimensional logarithmic fundamental frequency (log F0), 20-dimensional Mel-frequency cepstral coefficients (MFCCs), and 12-dimensional Constant-Q chromatogram (CQT).

<sup>1</sup>iMotions 2017. <https://imotions.com>

### Modality-specific Encoders

**Text Encoder:** For textual input processing, we employ BERT as the backbone encoder. The model supports both English (BERT-base-uncased) and Chinese (BERT-Chinese) variants depending on the dataset language. Text sequences are first tokenized using the BERT tokenizer, then fed into the pre-trained BERT model:

$$\mathbf{H}_t = \text{BERT}(\mathbf{U}_t) \in \mathbb{R}^{T \times d_{bert}}, \quad \mathbf{x}_t = \mathbf{H}_t[0, :] \in \mathbb{R}^{d_{bert}} \quad (B.1)$$

where  $\mathbf{U}_t$  represents the tokenized text input with shape  $(B, 3, T)$  containing input\_ids, attention\_mask, and token\_type\_ids,  $\mathbf{H}_t$  is the contextualized hidden states from BERT, and  $\mathbf{x}_t$  is the final text representation extracted from the [CLS] token. The text output dimension  $d_{bert} = 768$  is fixed across all datasets.

**Audio Encoder:** For acoustic feature processing, for the sake of efficiency, follow Self-MM (Yu et al. 2021), we utilize an LSTM-based subnet to capture temporal dependencies, which has few parameters:

$$\begin{aligned} \text{packed\_audio} &= \text{pack\_padded\_sequence}(\mathbf{U}_a, \text{lengths}), \\ \dots, (\mathbf{h}_{final}, \dots) &= \text{LSTM}(\text{packed\_audio}; \theta_a), \\ \mathbf{x}_a &= \text{Linear}(\text{Dropout}(\mathbf{h}_{final})) \end{aligned} \quad (B.2)$$

where  $\mathbf{U}_a \in \mathbb{R}^{T \times f_a}$  represents the input audio features, and  $\mathbf{x}_a \in \mathbb{R}^{d_{a.out}}$  is the final audio representation with  $d_{a.out} = 16$ .

**Visual Encoder:** Similar to the audio encoder, we employ the same subnet architecture to process visual feature sequences:

$$\begin{aligned} \text{packed\_video} &= \text{pack\_padded\_sequence}(\mathbf{U}_v, \text{lengths}), \\ \dots, (\mathbf{h}_{final}, \dots) &= \text{LSTM}(\text{packed\_video}; \theta_v), \\ \mathbf{x}_v &= \text{Linear}(\text{Dropout}(\mathbf{h}_{final})) \end{aligned} \quad (B.3)$$

where  $\mathbf{U}_v \in \mathbb{R}^{T \times f_v}$  represents the input visual features, and  $\mathbf{x}_v \in \mathbb{R}^{d_{v.out}}$  is the final visual representation with  $d_{v.out} = 32$ .

### Multimodal Feature Fusion

The extracted unimodal representations are concatenated and processed through a fusion network:

$$\begin{aligned} \mathbf{x}_{concat} &= \mathbf{x}_t \parallel \mathbf{x}_a \parallel \mathbf{x}_v, \\ \mathbf{h}_m &= \text{Dropout}(\text{ReLU}(W_1 \mathbf{x}_{concat} + b_1)) \end{aligned} \quad (B.5)$$

where the concatenated dimension is 816 (768+16+32), and  $\mathbf{h}_m \in \mathbb{R}^{128}$  is the fused representation.

### Dual Prediction Heads

**Regression Predictor:** Predicts continuous sentiment scores:

$$\hat{y}_s = W_r^{(2)} \text{ReLU}(W_r^{(1)} \mathbf{h}_m + b_r^{(1)}) + b_r^{(2)} \quad (B.6)$$

**Classification Predictor:** Performs 3-class sentiment classification:

$$\begin{aligned} \mathbf{z}_{cls} &= W_c^{(2)} \text{ReLU}(W_c^{(1)} \mathbf{h}_m + b_c^{(1)}) + b_c^{(2)}, \\ \mathbf{p}_s &= \text{Softmax}(\mathbf{z}_{cls}) \end{aligned} \quad (B.7)$$

## Training Objectives

The model is trained with a combined loss function:

$$\mathcal{L}_{total} = \text{MSE}(\hat{y}_s, y) + \text{CE}(\mathbf{p}_s, y_{cls}) \quad (\text{B.8})$$

where  $y_{cls}$  is the discretized sentiment label defined as:

$$y_{cls} = \begin{cases} 1 & (\text{Negative}), \quad y < 0 \\ 0 & (\text{Neutral}), \quad y = 0 \\ 2 & (\text{Positive}), \quad y > 0 \end{cases} \quad (\text{B.9})$$

## Uncertainty Estimation

During inference, uncertainty is computed as the entropy of the classification probability distribution:

$$u_s = - \sum_{i=1}^3 p_{s,i} \cdot \log(p_{s,i} + \epsilon) \quad (\text{B.10})$$

where  $\epsilon = 10^{-12}$  prevents numerical instability.

## Dataset-specific Configurations

The input feature dimensions and LSTM hidden sizes vary across datasets:

- **MOSI:** Feature dims: (768, 5, 20), LSTM hidden: audio=32, video=64
- **MOSEI:** Feature dims: (768, 74, 35), LSTM hidden: audio=32, video=32
- **SIMS:** Feature dims: (768, 33, 709), LSTM hidden: audio=16, video=64

## Optimization Strategy

UBM is trained using the Pytorch Framework. The model employs component-specific learning rates and weight decay values that vary across datasets. Table B.1 presents the detailed optimization parameters for each dataset.

Component	Parameter	MOSI	MOSEI	SIMS
BERT	Learning Rate	$5 \times 10^{-5}$	$5 \times 10^{-5}$	$5 \times 10^{-5}$
	Weight Decay	$1 \times 10^{-3}$	$1 \times 10^{-5}$	$1 \times 10^{-3}$
Audio LSTM	Learning Rate	$1 \times 10^{-3}$	$5 \times 10^{-3}$	$5 \times 10^{-3}$
	Weight Decay	$1 \times 10^{-3}$	0.0	$1 \times 10^{-2}$
Video LSTM	Learning Rate	$1 \times 10^{-4}$	$1 \times 10^{-3}$	$5 \times 10^{-3}$
	Weight Decay	$1 \times 10^{-3}$	0.0	$1 \times 10^{-2}$
Others	Learning Rate	$5 \times 10^{-4}$	$1 \times 10^{-3}$	$1 \times 10^{-3}$
	Weight Decay	$1 \times 10^{-3}$	$1 \times 10^{-2}$	$1 \times 10^{-3}$

Table B.1: Component-specific optimization configurations for each dataset.

All components use the Adam optimizer with component-specific parameter groups to enable fine-grained control over the training dynamics of different model parts.

## C Experimental Details and Additional Results

In this section, we provide additional experimental details and additional results, including a more comprehensive comparison between the proposed three uncertainty quantification methods, the ablation studies on CMU-MOSIE datasets. These results are consistent with the results on the main text, further demonstrating the effectiveness of the proposed method.

Dataset	Description	Acc7	Acc2	MAE
MOSEI	Prediction-Truth Difference	54.4	84.7	0.520
	Ensemble Variance	<u>55.2</u>	<b>86.4</b>	0.516
	<b>Ours</b>	<u>55.4</u>	<b>86.4</b>	<b>0.506</b>

Table B.2: Ablation experiments on CMU-MOSEI. Best results are in **bold**, second-best are underlined.

Method	Acc7 $\uparrow$	Acc2 $\uparrow$	F1 $\uparrow$	MAE $\downarrow$	Corr $\uparrow$
PTD	45.5	85.7	85.6	0.721	0.791
EV	43.6	84.5	84.4	0.743	0.784
<b>CBE</b>	<b>45.9</b>	<b>85.8</b>	<b>85.7</b>	<b>0.732</b>	<b>0.786</b>

Table B.3: Comparison of uncertainty quantification methods on CMU-MOSI dataset. PTD: Prediction-Truth Difference, EV: Ensemble Variance, CBE: Classification-based Entropy (Ours).

## D Prompt Design for MLLM Integration

### Dataset-specific Prompt Templates

**CH-SIMS v1 Dataset** *Sentiment scores range from -1 to +1, where -1 is highly negative, +1 is highly positive, and 0 is neutral. The speaker said '{text}'. What is the sentiment score of the person in the video based on visual, audio and text? Directly answer the sentiment score. Now, the model is required to re-predict the label of the incoming data, and at the same time, provide the results of uncertainty and predicted labels obtained by the BERT-based multimodal sentiment prediction model and MLLM: {data}.*

**CMU-MOSI and CMU-MOSEI Datasets** *Sentiment scores range from -3 to +3, where -3 is highly negative, +3 is highly positive, and 0 is neutral. The speaker said '{text}'. What is the sentiment score of the person in the video based on visual, audio and text? Directly answer the sentiment score. Now, the model is required to re-predict the label of the incoming data, and at the same time, provide the results of uncertainty and predicted labels obtained by the BERT-based multimodal sentiment prediction model and MLLM: {data}.*

### Template Variables

The prompt templates use the following variable substitutions:

- **{text}:** Transcribed text content from the video segment
- **{data}:** Structured data containing predictions and uncertainties from both UBM and MLLM models

### Design Principles

Our prompts follow a two-stage approach: (1) direct multimodal sentiment prediction, and (2) collaborative integration of both small and large model predictions with uncertainty estimates. Different sentiment scales are used: CH-SIMS uses a 7-point scale (-3 to +3), while MOSI/MOSEI use a continuous scale (-1 to +1).